Published OnlineFirst October 8, 2010; DOI: 10.1158/0008-5472.CAN-10-1251

Cancer Research

Therapeutic Targeting of TLR9 Inhibits Cell Growth and Induces Apoptosis in Neuroblastoma

Chiara Brignole[1], Danilo Marimpietri[1], Daniela Di Paolo[1], Patrizia Perri[1], Fabio Morandi[1], Fabio Pastorino[1], Alessia Zorzoli[1], Gabriella Pagnan[1], Monica Loi[1], Irene Caffa[1], Giovanni Erminio[2], Riccardo Haupt[2], Claudio Gambini[3], Vito Pistoia[1], and Mirco Ponzoni[1]

Abstract

The Toll-like receptor 9 (TLR9) evolved to cope with pathogens, but it is expressed in a variety of tumors for reasons that are unclear. In this study, we report that neuroblastoma (NB) cells express functional TLR9. Liposome-complexed CpG oligonucleotides inhibited the proliferation of TLR9-expressing NB cells and induced caspase-dependent apoptotic cell death. Inhibitory oligonucleotides (iODNs) abrogated these effects. RNA interference reduced TLR9 expression but not to the level where functional responses to CpG were abolished. Compared with free CpG, liposomal formulations of NB-targeted CpG (TL-CpG) significantly prolonged the survival of mice bearing NB tumor xenografts. While CpG alone lacked antitumor efficacy in NOD/SCID/IL2rg$^{-/-}$ mice, TL-CpG retained significant efficacy related to direct effects on tumor cells. TLR9 expression in primary human NB specimens was found to correlate inversely with disease stage. Our findings establish functional expression of TLR9 in NB and suggest that TLR9 may represent a novel theranostic target in this disease. *Cancer Res; 70(23); 9816–26. ©2010 AACR.*

Introduction

Toll-like receptors (TLRs) represent a family of highly conserved pattern recognition receptors, evolved by the immune system to recognize extracellular pathogen-associated motifs known as pathogen-associated molecular patterns (1). These are expressed predominantly by dendritic cells, macrophages, NK, and B cells. Recently, it has been reported that epithelial and endothelial cells (2, 3) as well various tumors, such as melanoma, colon, breast, prostate, and lung cancer (4, 5), can express TLRs. Although understanding of the functional impact of TLRs expression on tumor cells warrants further investigation, current evidence indicates that TLRs on cancer cells can either promote or inhibit tumor progression (4).

TLR9 recognizes unmethylated CpG dinucleotides, very common in bacterial DNA but not in vertebrate genome in which CpG are often methylated (6). Differently from most TLR members, expressed at the cell surface, TLR9 has cytoplasmic localization and resides in the endoplasmic reticulum (ER) of resting cells (6, 7). It has been shown that CpG DNA binds directly to TLR9. After internalization of CpG DNA into a subcellular lysosomal compartment, TLR9 translocates from ER to this CpG DNA–containing lysosomal compartment where TLR9/CpG DNA binding occurs and signal transduction is initiated (7). Synthetic CpG oligonucleotides (CpG ODNs) can be generated with specific CpG sequence motifs, as well as with backbone modifications. So far, 3 different classes of CpG ODN have been synthesized, differing each other in their ability to stimulate and activate different immune cell populations (8).

Neuroblastoma (NB) is the most common extracranial solid tumor of childhood; despite aggressive treatment approaches, the outcome for high-risk, NB-affected patients remains poor (9, 10). Thus, the identification of new molecular candidates to be developed as novel therapeutic targets represents a priority area of research.

We previously reported that the administration of liposomes targeted to NB cells via disialoganglioside GD_2 and encapsulating CpG-containing *c-myb*–specific antisense ODNs led to long-term survival of NB-bearing mice (11, 12).

On the basis of previous studies on the expression of TLRs on tumor cells of different lineages, including melanoma that shares the neuroectodermal origin with NB, we hypothesized that NB cells could express TLR9 and, consequently, respond to treatment with CpG DNA. Herein, we investigated the expression of TLR9 on a wide panel of NB cell lines and primary NB specimens and also assessed its functionality and mechanism of action.

This study shows for the first time, to our knowledge, the functional expression of TLR9 in NB and suggests that TLR9 may represent a novel prognostic and/or therapeutic target.

Authors' Affiliations: [1]Experimental Therapy Unit, Laboratory of Oncology, [2]Epidemiology and Biostatistics Section Scientific Directorate, and [3]Department of Pathology, G. Gaslini Children's Hospital, Genoa, Italy

Note: Supplementary material for this article is available at Cancer Research Online (http://cancerres.aacrjournals.org/).

C. Brignole and D. Marimpietri contributed equally to the work.

Corresponding Author: Chiara Brignole and Mirco Ponzoni, Experimental Therapy Unit, Laboratory of Oncology, G. Gaslini Children's Hospital, Largo Gerolamo Gaslini 5, 16148, Genoa, Italy. Phone: 0039-10-5636342; Fax: 0039-10-3779820. E-mail: chiarabrignole@ospedale-gaslini.ge.it and mircoponzoni@ospedale-gaslini.ge.it.

doi: 10.1158/0008-5472.CAN-10-1251

Published OnlineFirst October 8, 2010; DOI: 10.1158/0008-5472.CAN-10-1251

Materials and Methods

Liposomes preparation

Anti-GD_2–targeted CpG-entrapping liposomal formulation was prepared using the method already described by us for the tumor selective delivery of antisense ODNs (11, 13–15).

Cell lines and culture conditions

The human NB cell lines IMR-32, SH-SY5Y, SK-NSH, SK-NMC, SK-NAS, SK-NF-I, SK-NBE(2), and SK-NBE(2c) and the malignant B-cell line Raji were obtained from the American Type Culture Collection (Manassas, VA); the HTLA-230 cell line was a gift of Dr. E. Bogenmann (16) (Los Angeles Children's Hospital, CA); the other human NB cell lines GI-LI-N, GI-ME-N, ACN, LAN-1, LAN-5, and IMR-5 were obtained from the Biological Bank and Cell Factory (National Cancer Institute, Genoa, Italy). All cell lines were tested for mycoplasma contamination and characterized by cell proliferation, morphology evaluation, and multiplex short tandem repeat profiling test, both after thawing and within 8 passages in culture and used in this time frame.

Cells were grown in complete medium (Dulbecco's modified Eagle medium; Sigma), supplemented with 10% fetal bovine serum (Gibco-Invitrogen S.r.l., Carlsbad, CA) and 50 IU/mL of sodium penicillin G, 50 μg/mL of streptomycin sulfate, and 2 mmol/L of L-glutamine (all reagents from Sigma), as already described (17).

RNA isolation and gene expression analysis

The isolation of total RNA from cell lines was performed by chemical extraction in combination with a silica-based membrane immobilization, using QIAzol and RNeasy mini and micro kit (Qiagen, S.p.A., Milan, Italy). The mRNA expression levels of TLR9 target genes and the GAPDH-positive control were analyzed by a 2-step real-time quantitative PCR (qPCR) using a random priming-based reverse-transcription (High Capacity cDNA Reverse Transcription kit; Applied Biosystems, Austin, TX) and SYBR® Green I binding dye (Platinum® SYBR® Green qPCR SuperMix-UDG; Invitrogen S.r.l.), and data were normalized as previously reported (18).

The comparative Ct method was used for relative quantification of gene expression in wild-type and transfected cell lines. Analysis of the data was performed by qGene software (Biotechniques; ref. 19). (For details, see Supplementary Material.)

Cell proliferation assay

NB cells were plated, in quadruplicate for each treatment, in 96-well plates in complete medium, cultured for 24 hours, and then treated with CpG at a concentration of 4 μg/mL. Peripheral blood mononuclear cells (PBMNC) were treated immediately after isolation. CpG were administered to the cells either free or complexed with Lipofectamine™ RNA-iMAX (0.3 μL/well; Invitrogen S.r.l.) for additional 24 hours. Lipofectamine and CpG were complexed according to manufacturer's instruction. Hereafter, complexes formed by CpG and Lipofectamine™ RNA-iMAX will be referred to as L-CpG. As controls, the cells were also treated with L-ODN-scrambled (L-ODN-scr) at the same concentration of L-CpG and Lipofectamine alone. ^{3}H-Thymidine incorporation was quantified as described (20).

Cell viability assay

NB cells were cultured for 24 hours and then treated with CpG and L-CpG, as described previously, for additional 48 hours. At the end of treatment, the cells were harvested by scraping, washed with complete medium, and incubated with 0.4% trypan blue (1:1; Invitrogen) for 1 minute at 37°C. The cells were then counted using the Countess™ automated cell counter (Invitrogen S.r.l.) as reported (18, 20).

Apoptosis assays

Phosphatidyl serine detection. NB cells were plated and treated for 24 hours, as described earlier. Annexin V positivity was detected by the use of a human Annexin V-FITC kit (Bender MedSystems, Vienna, Austria), according to manufacturer's instructions (18, 20).

Caspase 3/7 activation. For the detection of caspase 3 and 7 cleavage activity, the Apo-ONE® Homogeneous Caspase 3–7 Assay was used (Promega, Madison, WI), according to manufacturer's instructions.

Mitochondrial membrane potential assay. The mitochondrial permeability transition event was evaluated using a MitoPT kit (Immunochemistry Technologies, LLC, Bloomington, MN) according to manufacturer's instructions as described (20). (For details, see Supplementary Material.)

Inhibition of TLR9 functionality

SH-SY5Y and GI-LI-N cells were seeded in 96-well plate [(7–9) × 10^3 cells/well)]. Class 2 inhibitory oligonucleotides (iODNs) [iODN (ttaggg)4 (TLRgrade™), Alexis Biochemicals)] were used to block TLR9 functionality. The cells were treated simultaneously with CpG (4 μg/mL) and iODN (20 μg/mL). In both cases, the administration was performed via Lipofectamine™ RNA-iMAX. The cells were observed after 48 hours, using a contrast-phase microscope (Olympus Optical Co Ltd, Tokyo, Japan) to define morphologic changes, and were photographed. Treated cells were also subjected to evaluation of cell proliferation at 24 hours, as described earlier.

Silencing of TLR9

NB and Raji cells were seeded in 6-well plate in complete medium. The day after, the cells were transfected with siRNA specific for TLR9 (Select Pre-Designed siRNA; Applied Biosystems/Ambion) for 14 hours in a serum-free medium. Three different sequences of Select Pre-designed siRNA were tested in silencing experiments; they will be referred hereafter as siRNA1-TLR9, siRNA2-TLR9, and siRNA3-TLR9. A siRNA specific for the housekeeping gene GAPDH (siRNA Custom; Applied Biosystems) and 1 siRNA negative control (Silencer Negative Control #1; Applied Biosystems) were also tested. For details on transfection and evaluation of efficiency of gene silencing, see Supplementary Material.

Western blot analysis

Protein lysates were prepared from various NB cell lines (GI-LI-N, SK-NAS, IMR-32, SH-SY5Y, HTLA-230, LAN-5, and

Published OnlineFirst October 8, 2010; DOI: 10.1158/0008-5472.CAN-10-1251

GI-ME-N) and from either untreated or treated siRNAs against TLR9, GI-LI-N, and HTLA-230 cells, as described (13). (For details, see Supplementary Material.)

In vivo therapeutic studies

All experiments involving animals were reviewed and approved by the licensing and ethical committee of the National Cancer Research Institute, Genoa, Italy, and by the Italian Ministry of Health. Five-week-old female, athymic (nude–nude), SCID-bg mice were purchased from Harlan Laboratories S.r.l. (S Pietro al Natisone, Italy). NOD/SCID/IL2rg$^{-/-}$ lacking the gene for the common gamma chain, a component of the receptor for IL2, and related cytokines were purchased from The Jackson Laboratory (Bar Harbor, ME). Mice were intravenously injected with 2.5×10^6 HTLA-230, as previously described (11). HTLA-230 NB cell lines have been chosen because they present high levels of both GD_2 and TLR9 and thus can be considered as a good target for *in vivo* studies. Mice were given intravenously injected with CpG (50 μg), either free or encapsulated within NB-targeted liposomes (TL-CpG). Control mice received HEPES-buffered saline. Treatment started 4 hours after cell challenge and continued for 2 weeks, 2 days per week, with a 3-day interval between courses. Mice were monitored and sacrificed when signs of poor health, such as abdominal dilatation, dehydration, or paraplegia, became evident.

Patients and collection of tumor samples

Fifty NB specimens at the onset, collected from 1987 to 2000, were retrieved from the Italian Neuroblastoma Tissue Bank by the Ethical Committee of the G. Gaslini Children's Hospital. All patients or their parents gave informed consent. Tumor cell content was consistently at least 80%, as assessed by histologic analysis. Disease extension was classified according to the International Neuroblastoma Staging System criteria (21). The specimens were from 10 patients with stage 1–2, age <12 months, 10 patients with stage 1–2, age >12 months, 10 patients with stage 4S, and 20 patients with stage 4 tumors (10 with no *MYCN* amplified and 10 *MYCN* amplified).

Immunohistochemistry

Immunohistochemical (IHC) analyses were performed using a staining method for sections of formalin-fixed, paraffin-embedded tissue on the Bond automated system (Vision BioSystems, Leica, Germany), as detailed in Supplementary Material.

Statistical analyses

All *in vitro* data are from at least 3 independent experiments. All the *in vivo* experiments were performed at least twice with similar results.

Results are expressed as mean ±95% confidence interval values for quantitative variables and as numbers and percentages for qualitative ones. For continuous variables, the statistical significance of differential findings between the experimental and control groups was determined by ANOVA with the Tukey multiple comparisons test. The association between categorical variables was assessed by the Fisher exact test. Survival curves were constructed using the Kaplan–Meier method and compared by the Peto log-rank test. Both ANOVA and log-rank tests were carried out using Graph-Pad Prism 3.0 software (Graph-Pad Software, Inc., El Camino Real, San Diego, CA). The remaining analyses were performed by Stata for Windows statistical package (release 9.2, Stata Corporation, College Station, TX). All tests were 2-sided and a value of $P < 0.05$ was considered as statistically significant.

Results

Effects of CpG on cell proliferation, cell death, and apoptosis

Data in Figure 1 show that NB cells express TLR9 at both mRNA and protein levels as assessed by real-time qPCR, flow cytometry, and Western blot analysis (Fig. 1A, B, and C, respectively).

Thus, to investigate the functionality of TLR9 in NB cells, PBMNC and NB cells were treated with CpG ODNs, at a concentration (4 μg/mL) already shown to be stimulatory on immunocompetent cells (22). CpG was delivered to cells either free (CpG) or via Lipofectamine™ RNA-iMAX (L-CpG), here used to allow the uptake of CpG into NB cells (23). Figure 2A shows that L-CpG stimulated cell proliferation of PBMNC but inhibited that of GI-LI-N NB cells. Free CpG showed activity only on PBMNC, likely due to the different membrane permeability of ODNs presented by cells of hematopoietic origin with respect to solid tumor-derived cells (23, 24). Furthermore, the effect of L-CpG was specific: indeed, either Lipofectamine alone or L-ODN-scr did not affect cell proliferation.

We then investigated whether L-CpG could also induce cell death. As shown in Figure 2B, only treatment with L-CpG induced GI-LI-N cell death whereas (L-CpG vs. control, $P < 0.001$) Lipofectamine or L-ODN-scr were not effective.

Cells treated with L-CpG displayed rounding up, retraction of pseudopods, reduction of cellular volume, and blebbing of the plasma membrane (Fig. 2C, left panel). All of these changes are hallmarks of apoptotic cells. The apoptotic cell death was further confirmed by an Annexin-V assay, in which Annexin-V binds to externalized phosphatidyl serine on the surface of apoptotic cells. As shown in Figure 2C, right panel, L-CpG–treated GI-LI-N contained a significantly higher percentage of Annexin V$^+$ apoptotic cells than control (L-CpG vs. control, $P < 0.001$). The addition of a pan-caspase inhibitor (Z-VAD-FMK) almost completely reverted the L-CpG–induced cell apoptosis (L-CpG vs. Z-VAD-FMK + L-CpG, $P < 0.01$), indicating the involvement of a caspase-dependent mechanism of programmed cell death. Supplementary Figure S1 shows the results obtained by treating IMR-32, GI-ME-N, HTLA-230, and LAN-5, as described earlier. As confirmed by the Annexin-V assay, all the cell lines tested responded to the treatment with L-CpG undergoing apoptosis.

We next investigated whether the administration of L-CpG induced cleavage of caspases 3 and 7. As clearly shown in Figure 2D, left panel, the treatment of GI-LI-N cells with L-CpG for 24 hours results in caspase 3 and 7 activation by cleavage. The proteasome inhibitor Bortezomib was used as the positive control (20). Pretreatment of NB cells with Z-VAD-FMK

Published OnlineFirst October 8, 2010; DOI: 10.1158/0008-5472.CAN-10-1251

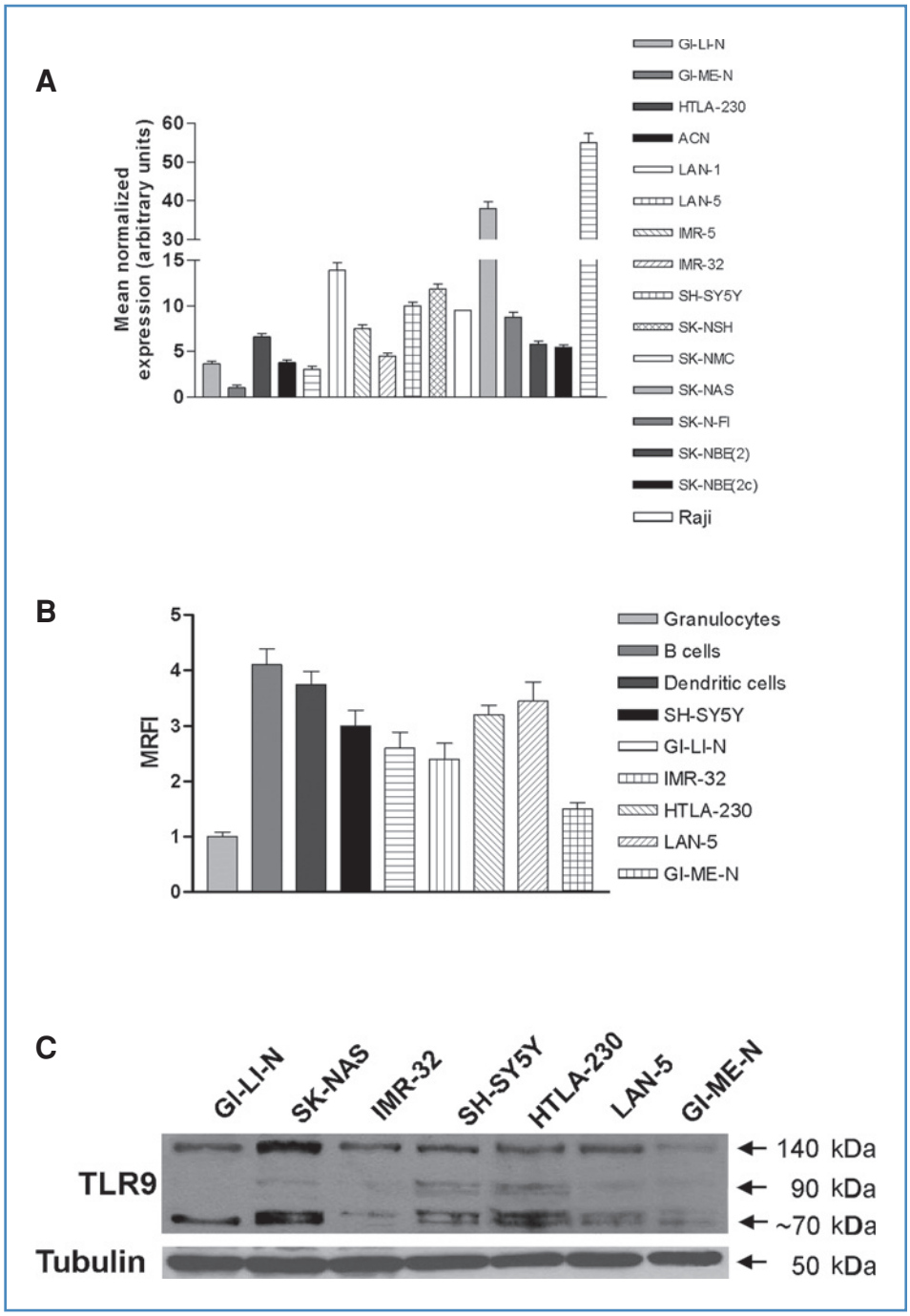

Figure 1. TLR9 expression in NB-cell lines. A, mRNA expression of TLR9, expressed as arbitrary units, was evaluated by real-time qPCR on Raji cells and neuroblastoma cell lines. B, intracellular protein expression of TLR9 was investigated by flow cytometry. The expression was defined as mean ratio fluorescence intensity (MRFI) over control (cells stained with an isotype-matched nonspecific Ab). MRFI equal to 1 means no expression. Experiments were performed in triplicate. C, TLR9 protein expression was investigated by Western blot analysis on a panel of NB-cell lines.

completely prevented CpG-induced caspase 3 and 7 cleavage. However, pretreatment of NB cells with the antioxidant *N*-acetyl-cysteine (NAC), an inhibitor of reactive oxygen species generation, was not effective in inhibiting caspase 3 and 7 cleavage.

Recently, caspases 3 and 7 have been reported to be key mediators of some mitochondrial events of apoptosis (25). Thus, we investigated whether the treatment of NB cells with L-CpG was associated with the activation of the intrinsic apoptotic signaling pathway. Treatment of GI-LI-N cells with L-CpG caused a statistically significant decrease in mitochondria membrane potential with respect to the control (L-CpG vs. control, $P < 0.01$; Fig. 2D, right panel). Pretreatment with either Z-VAD-FMK or NAC increased the percentage of cells with polarized mitochondria to the level of control. These results indicate that TLR9 triggering with CpG ODNs inhibits NB cell proliferation and induces cell death by apoptosis.

Published OnlineFirst October 8, 2010; DOI: 10.1158/0008-5472.CAN-10-1251

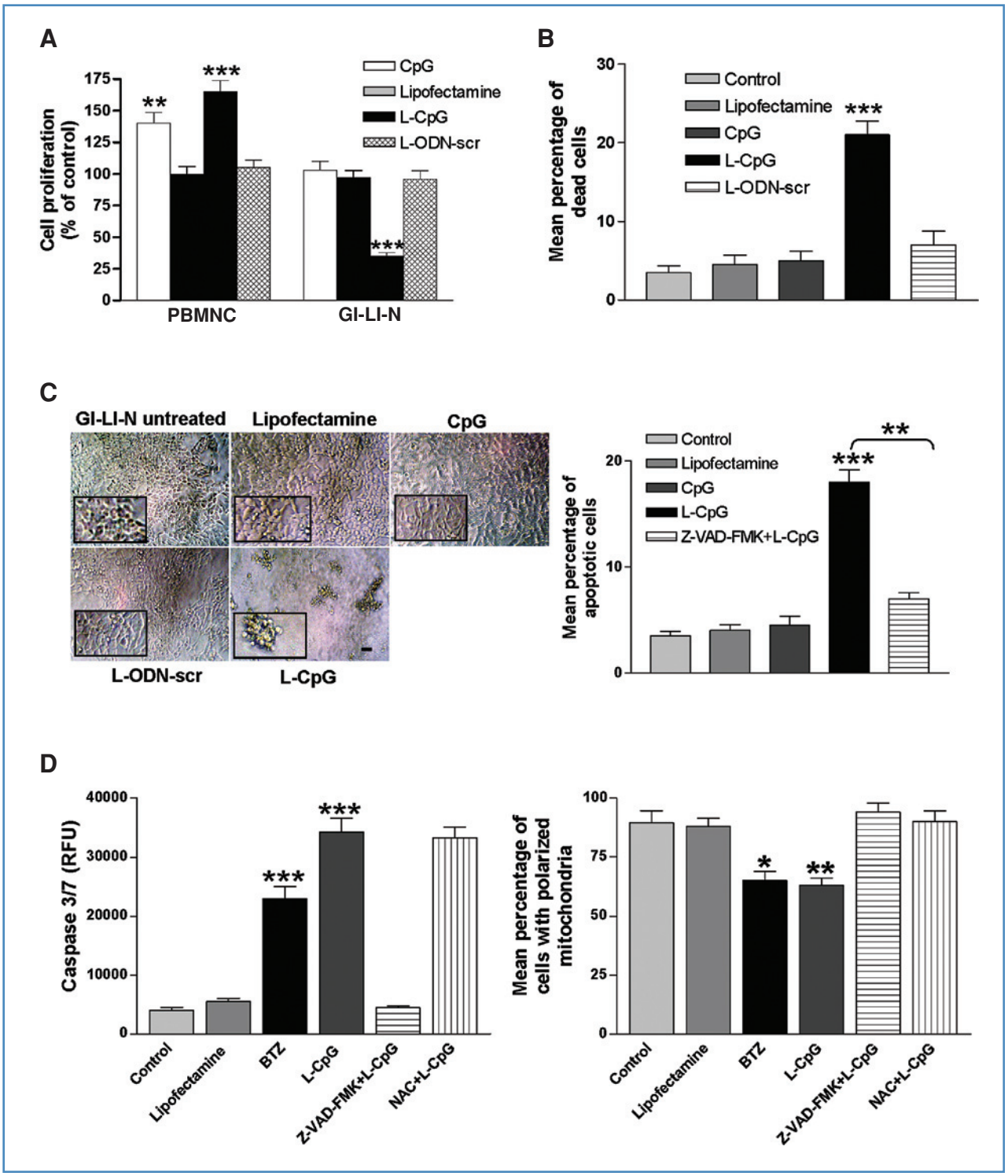

Figure 2. Effects of CpG on NB-cell lines. A, cell proliferation, defined as the percentage of control level, was determined in PBMNC and GI-LI-N cells after a 24-hour treatment with CpG alone, Lipofectamine alone, L-CpG, and L-ODN-scr. B, the mean percentage of dead GI-LI-N cells, treated as earlier, was determined by trypan blue dye exclusion assay. C, left, microphotographs representative of morphologic changes induced in GI-LI-N cells by treatment with L-CpG for 48 hours. Scale bar, 100 μm. C, right, mean percentage of apoptotic GI-LI-N cells was examined by the use of an Annexin-V FITC kit. D, left, caspase 3/7 activity was determined on GI-LI-N cells treated as earlier. Data are expressed as relative fluorescence unit (RFU). D, right, mitochondrial membrane potential was evaluated on GI-LI-N cells treated as earlier. In C and D, the antioxidant *N*-acetyl-cysteine (NAC) and the pan-caspase inhibitor Z-VAD-FMK were also used. In D, Bortezomib (BTZ) was used as a positive control for apoptosis induction. *, $P < 0.05$; **, $P < 0.01$; ***, $P < 0.001$.

Published OnlineFirst October 8, 2010; DOI: 10.1158/0008-5472.CAN-10-1251

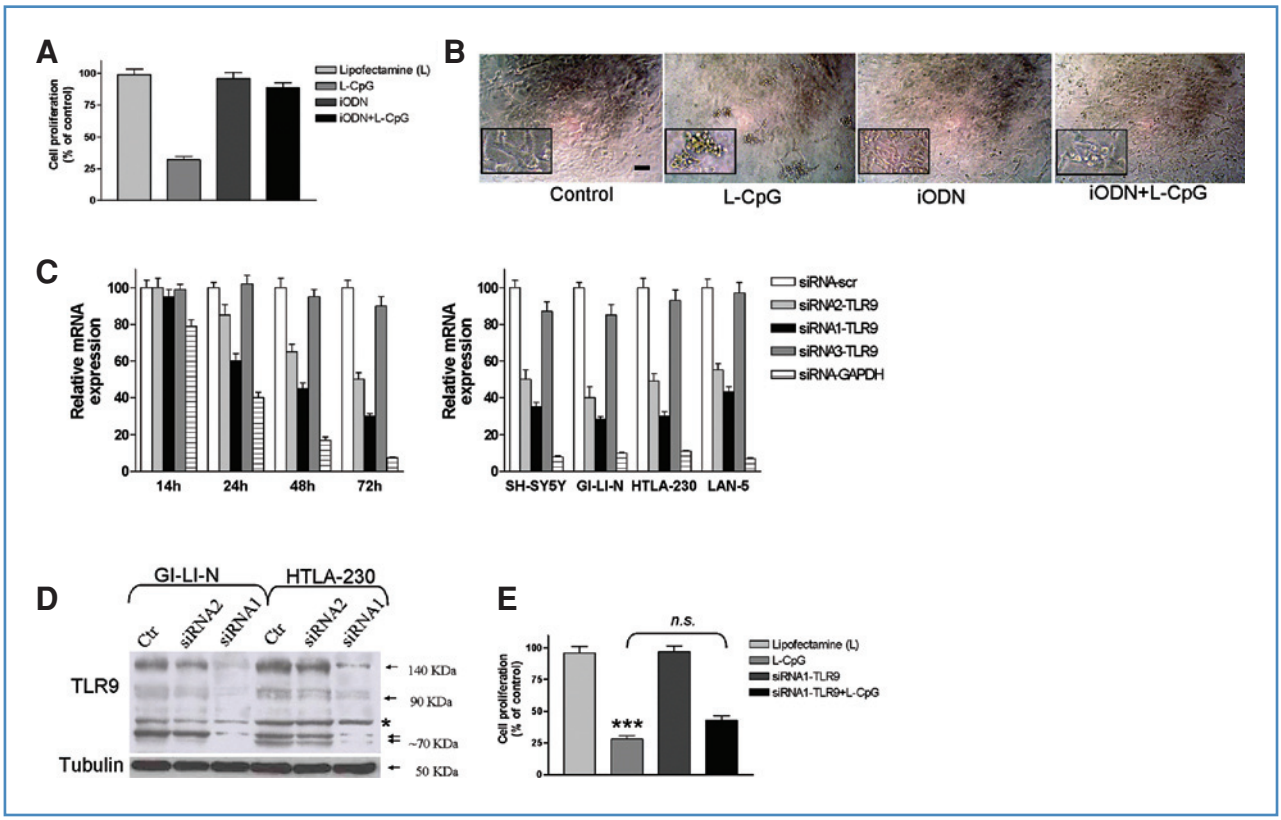

Figure 3. Silencing of TLR9 and inhibition of TLR9 functionality. A, SH-SY5Y cells were cotreated for 24 hours with L-CpG and iODN. Cell proliferation was assessed by ^{3}H-thymidine incorporation. B, microphotographs representative of morphologic changes induced on SH-SY5Y cells by the different treatments at 48 hours. Scale bar, 150 μm. C, TLR9 mRNA expression was evaluated after transfection with different siRNAs of Raji cells (left) and neuroblastoma cells (right), respectively. D, GI-LI-N and HTLA-230 cells were transfected for 72 hours with siRNA1 and siRNA2 specific for TLR9. The amount of TLR9 protein was determined by Western blot. *, not specific band. E, GI-LI-N cells transfected with siRNA1 were subjected to L-CpG treatment for further 24 hours. Cell proliferation was determined by ^{3}H-thymidine incorporation (*n.s.,* not significant; ***, $P < 0.001$).

TLR9 silencing and functionality

To show that the abrogation of TLR9 protein results in CpG ODN loss of efficacy, we tested iODNs. Class 2 iODNs used here are entirely composed of TTAGGG multimers designed both to block the colocalization of CpG ODNs with TLR9 within endosomal vesicles and to abrogate the signaling cascade downstream to TLR9 (26, 27). This suppressive activity correlates with the ability of TTAGGG motifs to form G-tetrads (26); these iODNs have been initially synthesized with the aim to block the activation of immune cells by CpG ODNs (28). They exert the inhibitory effect when administered in molar excess with respect to CpG ODNs. A 5-fold molar excess of iODN, with respect to L-CpG, could almost completely revert the antiproliferative effect obtained by the use of L-CpG on SH-SY5Y NB cells (iODN + L-CpG vs. L-CpG, $P < 0.01$; Fig. 3A). The iODN administered alone, as control, did not affect cell growth. Similar results were obtained for GI-LI-N cells (data not shown). These results are further supported by the findings shown in Figure 3B. Indeed, while SH-SY5Y cells treated with L-CpG underwent apoptotic cell death, cells cotreated with iODN, in molar excess with respect to L-CpG, had a morphologic aspect similar to untreated control cells.

Silencing experiments were also performed first on Raji cell to identify the more efficient TLR9-specific siRNA sequence and to determine the time point at which the highest TLR9 silencing was reached. As shown in Figure 3C, left panel, the GAPDH housekeeping gene was drastically silenced, in a time-dependent manner, reaching its maximum effect at 72 hours. Similarly, TLR9 silencing was time dependent. Nevertheless, a high silencing efficiency was not obtained for all the siRNA sequences used. Then, the 3 siRNA sequences were used to test their efficiency on a panel of NB cell lines. Also, in this case, the GAPDH gene was almost completely silenced at 72 hours (Fig. 3C, right panel), whereas the best sequence of siRNA against TLR9 (number 1) reduced TLR9 expression to about 60%. The silencing efficiency was further investigated by Western blot analysis. GI-LI-N and HTLA-230 cells were transfected with siRNA1-TLR9 and siRNA2-TLR9 and harvested at 72 hours. Both siRNA sequences failed to completely shutdown the expression of the expected full-length TLR9 protein (140 kDa; Fig. 3D), as well as of the cleaved isoforms (roughly 70–90 kDa). These last proteins have been reported recently to be functional also in macrophages (29). The expression of these low-molecular-weight isoforms has been confirmed in NB cells by a different antibody (Ab) against TLR9 (data not shown).

Published OnlineFirst October 8, 2010; DOI: 10.1158/0008-5472.CAN-10-1251

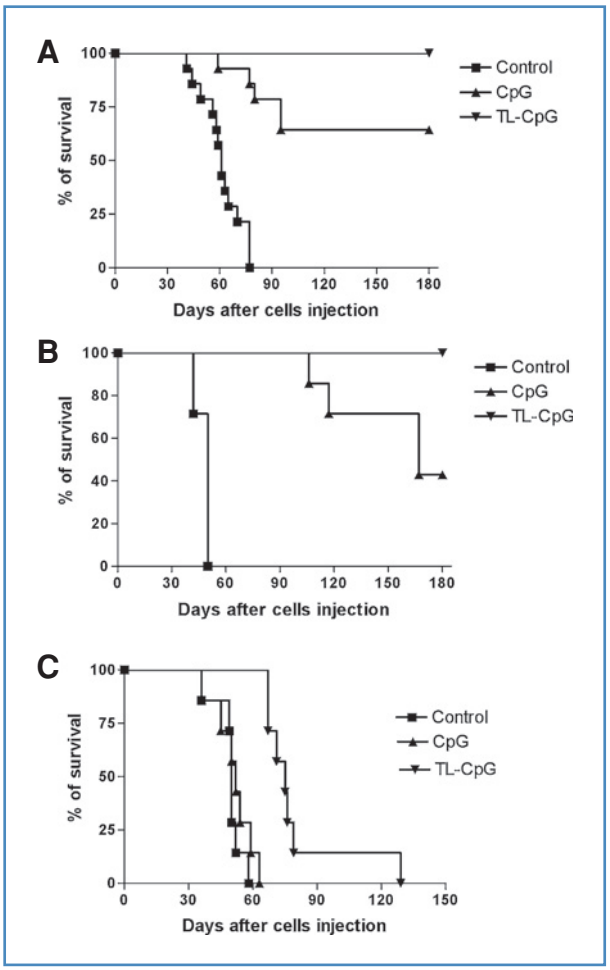

Figure 4. Survival curves of NB-bearing mice treated with TL-CpG: (A) Nude ($n = 14$), (B) SCID-bg ($n = 7$), and (C) NOD/SCID/IL2rg$^{-/-}$ ($n = 7$). Mice were injected with HTLA-230 NB cells into the tail vein and treated as reported in the Materials and Methods section.

Furthermore, as shown in Figure 3E, we showed that the amount of TLR9 protein remaining after silencing was still functional and sufficient to respond to L-CpG. Indeed, transfection of GI-LI-N cells for 72 hours with siRNA1-TLR9 only marginally reverted the inhibition of cell proliferation induced by a 24-hour treatment protocol with L-CpG.

These results clearly show that low-level expression of TLR9 in NB cells is sufficient to allow full functionality of this receptor.

In vivo effects of CpG

We next investigated whether CpG had antitumor activity in a biologically and clinically relevant pseudometastatic mouse model of human NB cell (11). The *in vitro* delivery of ODNs to solid tumor-derived cells is usually accomplished by carriers such as lipidic vesicles and cationic polymers (23, 24), whose utilization, in turn, can lead to *in vivo* limitations due mostly to the lack of specificity for target cells and some systemic toxicity (30, 31).

We have previously developed a standardized method to efficiently deliver ODNs to neuroectodermal tumors via disialoganglioside, GD_2 (13), which is abundantly expressed at the cell surface of NB cells whereas its expression in normal tissues is very limited (32). Monoclonal antibodies (mAbs) recognizing GD_2 bind to NB cells with high affinity and specificity and are rapidly internalized after binding, thus becoming an excellent tool for liposome-mediated tumor targeting (33). We therefore decided to use GD_2-targeted liposomes as vehicles for the *in vivo* intracellular delivery of CpG into GD_2^+ human NB cells. The high selectivity of this approach is guaranteed by the lack of GD_2 expression in any mouse tissue (34).

NB-targeted liposomes containing CpG (TL-CpG) were thus administered *in vivo* for therapeutic purposes. As shown in Figure 4A, both CpG and TL-CpG significantly prolonged the survival of tumor-bearing Nude mice ($P < 0.0001$). Interestingly, mice treated with TL-CpG lived longer than those treated with CpG ($P = 0.0154$), being all animals cured 6 months after NB-cell inoculation. This impressive antitumor effect obtained with TL-CpG is likely due to a dual attack of tumor cells. First, liposomal formulations containing CpG ODNs activate the host immune system to kill NB cells through a NK cell–dependent mechanism (11). Second, TL-CpG acts directly on NB cells binding to TLR9 and causes their apoptosis. In SCID-bg mice, lacking B and NK cells (11), similar results were unexpectedly obtained. Indeed, at 6 months after tumor challenge, animals treated with TL-CpG were all alive (TL-CpG vs. control, $P = 0.0004$) whereas about 40% of long-term survival was obtained for those treated with free CpG (Fig. 4B; TL-CpG vs. CpG, $P = 0.023$). Although in our previous work (11), administration of liposomal CpG-containing antisense ODNs to tumor-bearing SCID-bg mice lost its antitumor effectiveness, the present finding is in agreement with other studies showing that, upon activation with CpG, macrophages acquired cytotoxic potential against tumor cells (35). To definitively overcome the influence of the immune system in our therapeutic results, and to distinguish the direct effects of TL-CpG on tumor cells, we thus used NOD/SCID/IL2rg$^{-/-}$ mice. This mouse model lacks B and NK cells and presents macrophages with an impaired functionality (36). In this mouse model, treatment with CpG alone was completely ineffective with respect to control animals while TL-CpG treatment still maintained antitumor efficacy leading to an increased life span with respect to controls (Fig. 4C, $P = 0.0002$).

TLR9 expression in primary NB tumors

We analyzed 50 NB specimens at different stages by IHC analysis, as detailed in the Material and Methods section. NB specimens were scored as negative, weak, moderate, or strong with respect to the expression of TLR9.

Figure 5A,a and A,b shows a negative control stained with an isotype-matched irrelevant antibody and a TLR9-positive control, respectively, both from a pulmonary adenocarcinoma specimen. TLR9 positivity was graded by the intensity of cytoplasmic staining. Panels A,c to A,f show representative micrographs of TLR9 expression in NB specimens. Specifically, panel A,c is negative for TLR9 expression and representative of a stage 4, *MYCN*-amplified tumor. Panel A,e shows weak TLR9 expression in a stage 4, *MYCN* nonamplified tumor. Panel A,f shows moderate TLR9 expression in a stage 4S patient and,

Published OnlineFirst October 8, 2010; DOI: 10.1158/0008-5472.CAN-10-1251

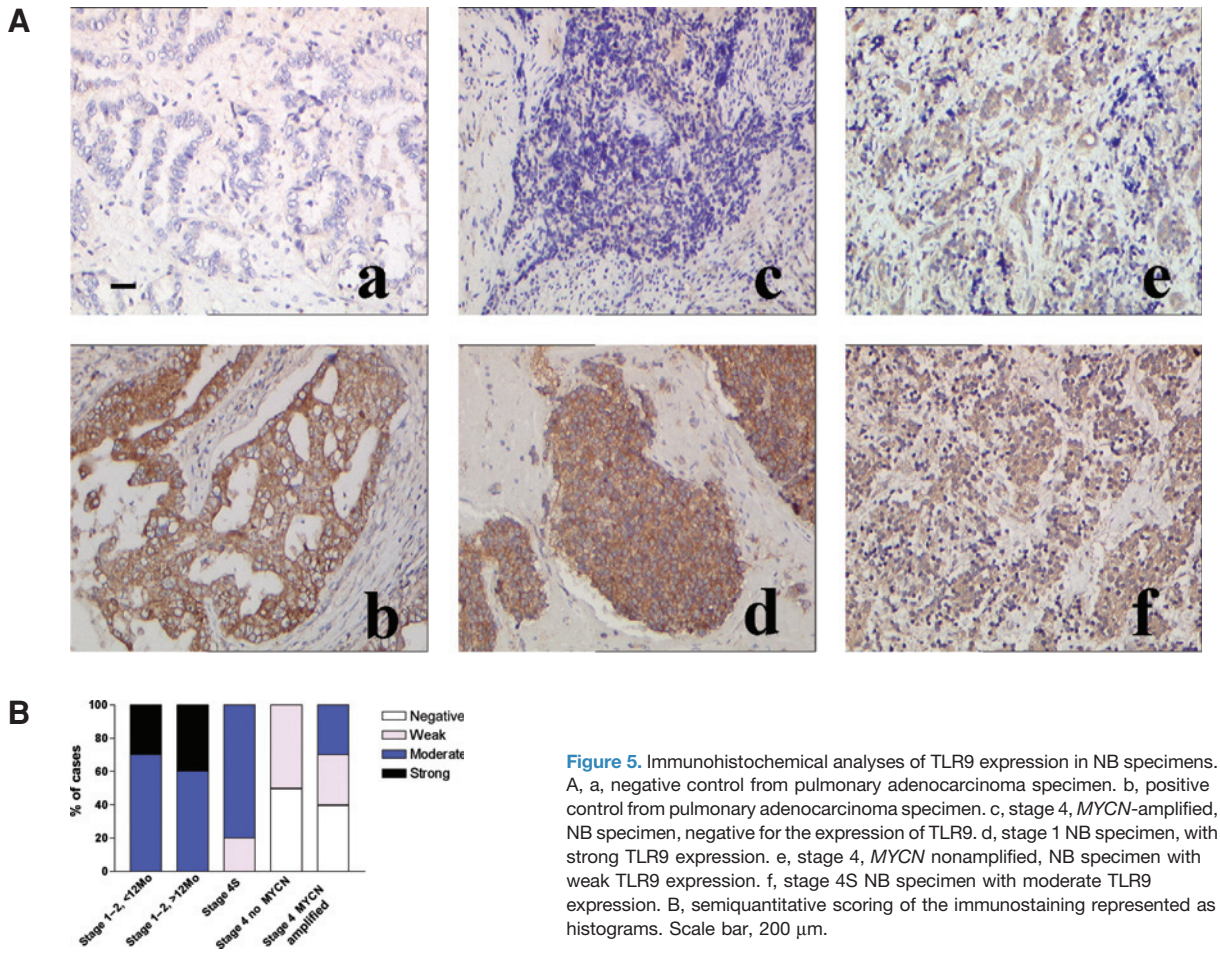

Figure 5. Immunohistochemical analyses of TLR9 expression in NB specimens. A, a, negative control from pulmonary adenocarcinoma specimen. b, positive control from pulmonary adenocarcinoma specimen. c, stage 4, *MYCN*-amplified, NB specimen, negative for the expression of TLR9. d, stage 1 NB specimen, with strong TLR9 expression. e, stage 4, *MYCN* nonamplified, NB specimen with weak TLR9 expression. f, stage 4S NB specimen with moderate TLR9 expression. B, semiquantitative scoring of the immunostaining represented as histograms. Scale bar, 200 μm.

finally, panel A,d represents strong TLR9 expression from a stage 1 tumor.

Histogram representation (Fig. 5B) gives a semiquantitative scoring of the immunostaining, assessed by the Quick Score method, adapted from commonly used method for breast carcinomas (37). This panel clearly shows that the expression of TLR9 is inversely related to the stage of the disease. Indeed, the highest expression of TLR9 is present in stage 1–2 and stage 4S NB patients whereas about 50% of stage 4 patients are completely negative. The association between TLR9 and clinicopathologic features is also illustrated in Table 1. High TLR9 expression was prevalent in stage 1–2 (100%) and stage 4S (80%) patients, whereas much lower TLR9 expression was observed in the stage 4 group (85%, $P < 0.0001$). Furthermore, high TLR9 expression was associated with low age at diagnosis ($P = 0.018$) and normal *MYCN* status ($P = 0.030$).

Discussion

The significance of TLR9 expression and its biological impact in tumor cells is yet to be completely understood. The aim of this study was to investigate expression, functionality, and biological relevance of TLR9 in NB. Here, we showed, for the first time to our knowledge, that NB cells express TLR9, both at the mRNA and protein levels. In this respect, a previous report showed that human NB cells also express an intracellular form of TLR4 (38).

Previous reports indicate that triggering of TLR9 expressed by different malignant cells could lead to opposite effects, that is, stimulation of tumor progression or inhibition of tumor growth (4). Indeed, in TLR9-expressing human prostate cancer cells (39), treatment with CpG damped tumor growth and proliferation and induced apoptosis whereas it prolonged the survival of glioma-bearing mice (40). Moreover, Ren et al. (41) showed that human lung cancer cells expressed functional TLR9 and its stimulation enhanced their metastatic potential.

In this article, we show that TLR9 expression has a functional impact on NB cell growth, as stimulation of this receptor with CpG triggered tumor cell death. The latter was attributable to apoptosis, as shown by the involvement of caspases 3 and 7. Because apoptosis may occur through the activation of a different and independent pathway, we also investigated

Published OnlineFirst October 8, 2010; DOI: 10.1158/0008-5472.CAN-10-1251

Table 1. Association between clinicopathologic variables and TLR9 expression in 50 neuroblastoma patients

Variable	TLR9 expression[a]				P^b
	Low ($n = 19$)		High ($n = 31$)		
	N	%	*N*	%	
Stage[c]					<0.0001
1–2	0	0.0	20	100	
4S	2	20.0	8	80.0	
4	17	85.0	3	15.0	
Age, mo					0.018
<12	4	18.2	18	81.8	
>12	15	53.6	13	46.4	
MYCN					0.030
Amplified	12	30.0	28	70.0	
Nonamplified	7	70.0	3	30.0	

[a]TLR9 expression was dichotomized into low (score negative + weak) and high (moderate + strong) groups for analysis.
[b]The Fisher exact test (2-sided).
[c]From International Neuroblastoma Staging System (21).

mitochondrial cell death. Indeed, the treatment of NB cells with CpG resulted in the depolarization of mitochondrial membrane potential; this event is thought to contribute to cell death through the disruption of the normal function of mitochondria (42). Although caspases 3 and 7 have been so far considered as effector caspases downstream to mitochondrial related apoptosis, it was recently reported that these caspases are crucial for apoptotic cell death (25). We found that pretreatment of NB cells with a pan-caspase inhibitor prevented CpG-induced caspase 3 and 7 cleavage activation as well as the depolarization of mitochondrial membrane potential. Nevertheless, the use of the antioxidant NAC prevented mitochondrial membrane depolarization but not caspase 3 and 7 activation. These findings are consistent with a previous report (25) showing that caspases 3 and 7 work upstream of the mitochondrial pathway and suggest that free radicals could be one of the intermediate in this pathway of apoptosis.

The functionality of TLR9 in NB was further proved with experiments in which iODNs abrogated CpG-mediated apoptosis. Silencing experiments were also performed to support this finding. However, none of the 3 TLR9-specific siRNA sequences completely abrogated TLR9 expression. This finding is consistent with a recent report in which investigators, by using RNA interference, downregulated only partially the expression of TLR9 in dendritic cells. Nevertheless, such downregulation was sufficient to abrogate the effects of CpG ODNs in the induction of dendritic cells maturation (43). In contrast, we observed that all NB-cell lines transfected with siRNA against TLR9 retained the ability to respond to CpG, undergoing apoptosis. Thus, also NB cells expressing very low amount of TLR9 may be responsive to treatment with CpG ODNs. This conclusion is supported by the lack of correlation between TLR9 expression and apoptotic response to L-CpG observed in the various NB cell lines, further underlining that a very little TLR9 seems to be needed for maximal CpG responses.

In vivo experiments were performed in a biologically and clinically relevant mouse model of human NB (11). Because the most frequently used DNA carriers lack specificity to target cells, we have generated tumor-targeted delivery of CpG ODNs, specific for NB cells via anti-GD_2–targeted stealth liposomes (herein called TL-CpG), which have been shown to be the most efficient and safe envelop packaged way to transfer nucleic acid into neuroectodermal tumors cells (11, 13).

TL-CpG showed higher antitumor effect in NB animal models than CpG, becoming a candidate for further clinical development. In the last few years, nanomedicine has turned into a rapid growth research area, particularly for anticancer applications. Several nanomedicines, primarily lipid-based drug carriers such as DOXIL/Caelyx (Ortho Biotech; Janssen Pharmaceutical Companies), have received clinical approval and several lipid-based and polymeric carriers are undergoing clinical evaluation (44). A logical extension of this success is to further improve the antitumor effects of liposomal nanomedicines in a more selective manner through the use of ``active-targeting moieties'' coupled to their external surface. Receptor-mediated internalization of nanomedicines into tumor cells is mandatory for improved therapeutic efficacy of targeted liposomal drugs (45). In this regard, the disialoganglioside GD_2 is an internalizing receptor selectively expressed by neuroectoderma-derived tumor cells only of human origin (32–34, 46, 47), including the HTLA-230 cell line used in this study. Our results indicated that liposomal CpG could enter into the NB cells when targeted via the anti-GD_2 mAb coupled at the external surface of the nanoparticles but not in the absence

Published OnlineFirst October 8, 2010; DOI: 10.1158/0008-5472.CAN-10-1251

of the targeting agent, as already shown for antisense ODNs and different antitumor drugs (11, 13). These results support the direct effect of CpG on TLR9 expressed by NB cells.

TL-CpG triggered long-term survival of NB-bearing Nude mice, which was significantly superior to that achieved by administering CpG alone. This result could be due to a dual mechanism of action of TL-CpG. Indeed, liposomes containing CpG ODNs can also work as activators of the immune system, giving rise to a cascade of events that culminate in the activation of NK cells and consequent tumor cells killing carried out by NK cells themselves (11). Furthermore, CpG and TL-CpG both showed efficacy in SCID-bg mice, even if at different extent, confirming the implication of the immune system in the antitumor result. Because SCID-bg mice lack B and NK cells, our data could be explained by macrophage intervention upon activation with CpG (35). The definitive abrogation of immune system implication in therapeutic results was obtained by the use of NOD/SCID/IL2rg$^{-/-}$, which besides NK- and B-cell deficiency further presents the myeloid lineage with an impaired functionality (48). Indeed, it has been suggested that macrophages in NOD mice are functionally immature. As expected, the only effective treatment in this model was TL-CpG, which led to an increased life span. Thus, the potent antitumor effect of TL-CpG also seems to be due to a direct antitumor effect of CpG on NB cells, which, as shown in this study, express TLR9 as a functional intracellular ``death receptor.''

Investigations of TLR9 expression in NB patients have highlighted an inverse correlation between the stage of the disease and the levels of TLR9 expression ($P < 0.0001$). Low stages of NB disease are indeed characterized by moderate-to-strong TLR9 expression, whereas high stages are either negative or weakly/moderately positive. The strong expression of TLR9 in stage 4S and stage 1–2 tumors from patients younger than 12 months may hypothesize that TLR9 could be one of the molecules involved in transdifferentiation, apoptosis, and/or spontaneous regression of low-stage NB (9, 10). This hypothesis may be supported by the correlation between high TLR9 expression and age younger than 12 months ($P = 0.018$). In contrast, NB cells lacking TLR9 (advanced stages) may be prone to tumor progression.

Studies are ongoing to verify, in larger cohort of NB patients, whether the expression of TLR9 correlates also with the outcome of the disease. In such case, TLR9 could become a new prognostic marker for NB.

In conclusion, this study showed for the first time that TLR9 is expressed by NB, is functional, and has a biological impact on tumor growth, thus suggesting that TLR9 can be considered as a new molecular target for NB treatment.

Disclosure of Potential Conflict of Interest

No potential conflicts of interest were disclosed.

Acknowledgments

We thank Stefano Parodi for helpful discussion and Manuela Ferraro for the preparation of neuroblastoma specimen sections.

Grant Support

This work was supported by Associazione Italiana Ricerca Cancro and Italian Ministry of Health. D. Di Paolo is the recipient of Fondazione Italiana Ricerca Cancro fellowship.

Received 04/26/2010; revised 09/10/2010; accepted 09/22/2010; published OnlineFirst 10/08/2010.

References

1. Iwasaki A, Medzhitov R. Toll-like receptor control of the adaptive immune responses. Nat Immunol 2004;5:987–95.
2. Hornef MW, Bogdan C. The role of epithelial Toll-like receptor expression in host defense and microbial tolerance. J Endotoxin Res 2005;11:124–8.
3. Schmausser B, Andrulis M, Endrich S, Lee SK, Josenhans C, Muller-Hermelink HK, et al. Expression and subcellular distribution of toll-like receptors TLR4, TLR5 and TLR9 on the gastric epithelium in *Helicobacter pylori* infection. Clin Exp Immunol 2004;136: 521–6.
4. Zeromski J, Mozer-Lisewska I, Kaczmarek M. Significance of Toll-like receptors expression in tumor growth and spreading: a short review. Cancer Microenviron 2008;1:37–42.
5. Huang B, Zhao J, Li H, He KL, Chen Y, Chen SH, et al. Toll-like receptors on tumor cells facilitate evasion of immune surveillance. Cancer Res 2005;65:5009–14.
6. Krieg AM. Therapeutic potential of toll-like receptor 9 activation. Nat Rev Drug Discov 2006;5:471–84.
7. Latz E, Schoenemeyer A, Visintin A, Fitzgerald KA, Monks BG, Knetter CF, et al. TLR9 signals after translocating from the ER to CpG DNA in the lysosome. Nat Immunol 2004;5:190–8.
8. Vollmer J, Krieg AM. Immunotherapeutic applications of CpG oligodeoxynucleotide TLR9 agonists. Adv Drug Deliv Rev 2009;61: 195–204.
9. Brodeur GM. Neuroblastoma: biological insights into a clinical enigma. Nat Rev Cancer 2003;3:203–16.
10. Maris JM, Hogarty MD, Bagatell R, Cohn SL. Neuroblastoma. Lancet 2007;369:2106–20.
11. Brignole C, Pastorino F, Marimpietri D, Pagnan G, Pistorio A, Allen TM, et al. Immune cell-mediated antitumor activities of GD2-targeted liposomal c-myb antisense oligonucleotides containing CpG motifs. J Natl Cancer Inst 2004;96:1171–80.
12. Brignole C, Marimpietri D, Pastorino F, Di Paolo D, Pagnan G, Loi M, et al. Anti-IL-10R antibody improves the therapeutic efficacy of targeted liposomal oligonucleotides. J Control Release 2009; 138:122–7.
13. Pagnan G, Stuart DD, Pastorino F, Raffaghello L, Montaldo PG, Allen TM, et al. Delivery of c-myb antisense oligodeoxynucleotides to human neuroblastoma cells via disialoganglioside GD(2)-targeted immunoliposomes: antitumor effects. J Natl Cancer Inst 2000; 92:253–61.
14. Stuart DD, Allen TM. A new liposomal formulation for antisense oligodeoxynucleotides with small size, high incorporation efficiency and good stability. Biochim Biophys Acta 2000;1463:219–29.
15. Pastorino F, Brignole C, Marimpietri D, Pagnan G, Morando A, Ribatti D, et al. Targeted liposomal c-myc antisense oligodeoxynucleotides induce apoptosis and inhibit tumor growth and metastases in human melanoma models. Clin Cancer Res 2003;9:4595–605.
16. Bogenmann E. A metastatic neuroblastoma model in SCID mice. Int J Cancer 1996;67:379–85.

Published OnlineFirst October 8, 2010; DOI: 10.1158/0008-5472.CAN-10-1251

17. Ponzoni M, Bocca P, Chiesa V, Decensi A, Pistoia V, Raffaghello L, et al. Differential effects of *N*-(4-hydroxyphenyl)retinamide and retinoic acid on neuroblastoma cells: apoptosis versus differentiation. Cancer Res 1995;55:853–61.
18. Marimpietri D, Brignole C, Nico B, Pastorino F, Pezzolo A, Piccardi F, et al. Combined therapeutic effects of vinblastine and rapamycin on human neuroblastoma growth, apoptosis, and angiogenesis. Clin Cancer Res 2007;13:3977–88.
19. Muller PY, Janovjak H, Miserez AR, Dobbie Z. Processing of gene expression data generated by quantitative real-time RT-PCR. Biotechniques 2002;32:1372–4, 6, 8–9.
20. Brignole C, Marimpietri D, Pastorino F, Nico B, Di Paolo D, Cioni M, et al. Effect of Bortezomib on human neuroblastoma cell growth, apoptosis, and angiogenesis. J Natl Cancer Inst 2006;98:1142–57.
21. Brodeur GM, Pritchard J, Berthold F, Carlsen NL, Castel V, Castelberry RP, et al. Revisions of the international criteria for neuroblastoma diagnosis, staging, and response to treatment. J Clin Oncol 1993;11:1466–77.
22. Bauer S, Kirschning CJ, Hacker H, Redecke V, Hausmann S, Akira S, et al. Human TLR9 confers responsiveness to bacterial DNA via species-specific CpG motif recognition. Proc Natl Acad Sci U S A 2001;98:9237–42.
23. Corrias MV, Guarnaccia F, Ponzoni M. Bioavailability of antisense oligonucleotides in neuroblastoma cells: comparison of efficacy among different types of molecules. J Neurooncol 1997;31: 171–80.
24. Giles RV, Spiller DG, Grzybowski J, Clark RE, Nicklin P, Tidd DM. Selecting optimal oligonucleotide composition for maximal antisense effect following streptolysin *O*-mediated delivery into human leukaemia cells. Nucleic Acids Res 1998;26:1567–75.
25. Lakhani SA, Masud A, Kuida K, Porter GA Jr., Booth CJ, Mehal WZ, et al. Caspases 3 and 7: key mediators of mitochondrial events of apoptosis. Science 2006;311:847–51.
26. Gursel I, Gursel M, Yamada H, Ishii KJ, Takeshita F, Klinman DM. Repetitive elements in mammalian telomeres suppress bacterial DNA-induced immune activation. J Immunol 2003;171:1393–400.
27. Murchie AI, Lilley DM. Tetraplex folding of telomere sequences and the inclusion of adenine bases. EMBO J 1994;13:993–1001.
28. Yamada H, Gursel I, Takeshita F, Conover J, Ishii KJ, Gursel M, et al. Effect of suppressive DNA on CpG-induced immune activation. J Immunol 2002;169:5590–4.
29. Ewald SE, Lee BL, Lau L, Wickliffe KE, Shi GP, Chapman HA, et al. The ectodomain of Toll-like receptor 9 is cleaved to generate a functional receptor. Nature 2008;456:658–62.
30. Higuchi Y, Kawakami S, Oka M, Yamashita F, Hashida M. Suppression of TNFalpha production in LPS induced liver failure in mice after intravenous injection of cationic liposomes/NFkappaB decoy complex. Pharmazie 2006;61:144–7.
31. Howard KA, Rahbek UL, Liu X, Damgaard CK, Glud SZ, Andersen MO, et al. RNA interference *in vitro* and *in vivo* using a novel chitosan/siRNA nanoparticle system. Mol Ther 2006;14:476–84.
32. Mujoo K, Cheresh DA, Yang HM, Reisfeld RA. Disialoganglioside GD2 on human neuroblastoma cells: target antigen for monoclonal antibody-mediated cytolysis and suppression of tumor growth. Cancer Res 1987;47:1098–104.
33. Wargalla UC, Reisfeld RA. Rate of internalization of an immunotoxin correlates with cytotoxic activity against human tumor cells. Proc Natl Acad Sci U S A 1989;86:5146–50.
34. Lode HN, Xiang R, Varki NM, Dolman CS, Gillies SD, Reisfeld RA. Targeted interleukin-2 therapy for spontaneous neuroblastoma metastases to bone marrow. J Natl Cancer Inst 1997;89:1586–94.
35. Wu QL, Buhtoiarov IN, Sondel PM, Rakhmilevich AL, Ranheim EA. Tumoricidal effects of activated macrophages in a mouse model of chronic lymphocytic leukemia. J Immunol 2009;182:6771–8.
36. Serreze DV, Gaedeke JW, Leiter EH. Hematopoietic stem-cell defects underlying abnormal macrophage development and maturation in NOD/Lt mice: defective regulation of cytokine receptors and protein kinase C. Proc Natl Acad Sci U S A 1993;90:9625–9.
37. Detre S, Saclani Jotti G, Dowsett M. A `quickscore'' method for immunohistochemical semiquantitation: validation for oestrogen receptor in breast carcinomas. J Clin Pathol 1995;48:876–8.
38. Hassan F, Islam S, Tumurkhuu G, Naiki Y, Koide N, Mori I, et al. Intracellular expression of toll-like receptor 4 in neuroblastoma cells and their unresponsiveness to lipopolysaccharide. BMC Cancer 2006;6:281.
39. Rayburn ER, Wang W, Zhang Z, Li M, Zhang R, Wang H. Experimental therapy of prostate cancer with an immunomodulatory oligonucleotide: effects on tumor growth, apoptosis, proliferation, and potentiation of chemotherapy. Prostate 2006;66:1653–63.
40. El Andaloussi A, Sonabend AM, Han Y, Lesniak MS. Stimulation of TLR9 with CpG ODN enhances apoptosis of glioma and prolongs the survival of mice with experimental brain tumors. Glia 2006;54: 526–35.
41. Ren T, Wen ZK, Liu ZM, Liang YJ, Guo ZL, Xu L. Functional expression of TLR9 is associated to the metastatic potential of human lung cancer cell: functional active role of TLR9 on tumor metastasis. Cancer Biol Ther 2007;6:1704–9.
42. van Loo G, Saelens X, Matthijssens F, Schotte P, Beyaert R, Declercq W, et al. Caspases are not localized in mitochondria during life or death. Cell Death Differ 2002;9:1207–11.
43. Ma L, Zhao G, Hua C, Li X, Zhao X, Sun L, et al. Down-regulation of TLR9 expression affects the maturation and function of murine bone marrow-derived dendritic cells induced by CpG. Cell Mol Immunol 2009;6:199–205.
44. Allen TM, Cheng WW, Hare JI, Laginha KM. Pharmacokinetics and pharmacodynamics of lipidic nano-particles in cancer. Anticancer Agents Med Chem 2006;6:513–23.
45. Sapra P, Allen TM. Internalizing antibodies are necessary for improved therapeutic efficacy of antibody-targeted liposomal drugs. Cancer Res 2002;62:7190–4.
46. Pastorino F, Di Paolo D, Piccardi F, Nico B, Ribatti D, Daga A, et al. Enhanced antitumor efficacy of clinical-grade vasculature-targeted liposomal doxorubicin. Clin Cancer Res 2008;14:7320–9.
47. Pastorino F, Brignole C, Di Paolo D, Nico B, Pezzolo A, Marimpietri D, et al. Targeting liposomal chemotherapy via both tumor cell-specific and tumor vasculature-specific ligands potentiates therapeutic efficacy. Cancer Res 2006;66:10073–82.
48. Wagner-Ballon O, Chagraoui H, Prina E, Tulliez M, Milon G, Raslova H, et al. Monocyte/macrophage dysfunctions do not impair the promotion of myelofibrosis by high levels of thrombopoietin. J Immunol 2006;176:6425–33.

Cancer Research
The Journal of Cancer Research (1916–1930) | The American Journal of Cancer (1931–1940)

AACR American Association for Cancer Research

Therapeutic Targeting of TLR9 Inhibits Cell Growth and Induces Apoptosis in Neuroblastoma

Chiara Brignole, Danilo Marimpietri, Daniela Di Paolo, et al.

Cancer Res 2010;70:9816-9826. Published OnlineFirst October 8, 2010.